Published in final edited form as:
Biochemistry. 2008 November 11; 47(45): 11869–11876. doi:10.1021/bi8014828.

Large changes in the CRAC segment of the gp41 of HIV does not destroy fusion activity if the segment interacts with cholesterol

Sundaram A. Vishwanathan[⊥,1], **Annick Thomas**[+,1], **Robert Brasseur**[+], **Raquel F. Epand**[§], **Eric Hunter**[⊥], and **Richard M. Epand**[§]

⊥*Emory Vaccine Research Center, Yerkes, Emory University, 954 Gatewood Rd, Atlanta, GA 30329 U.S.A.*

§*Department of Biochemistry and Biomedical Sciences, McMaster University, 1200 Main Street West, Hamilton, Ontario L8N 3Z5 Canada*

+*Faculté Universitaire des Sciences Agronomiques de Gembloux Centre de Biophysique Moléculaire Numérique, Passage des Déportés, 2 5030 Gembloux, Belgium*

Abstract

The membrane-proximal external region (MPER) of the gp41 fusion protein of HIV is highly conserved among isolates of this virus and is considered a target for vaccine development. This region also appears to play a role in membrane fusion as well as localization of the virus to cholesterol-rich domains in membranes. The carboxyl terminus of MPER has the sequence LWYIK and appears to have an important role in cholesterol interactions. We have tested how amino acid substitutions that would affect the conformational flexibility of this segment could alter its interaction with cholesterol. We studied a family of peptides (all peptides as N-acetyl-peptide amides) with P, G or A substituting for W and I of LWYIK. The peptide having the largest effect on cholesterol distribution in membranes was the most flexible one, LGYGK. The corresponding mutation in gp41 resulted in a protein retaining 72% of the fusion activity of the wild type protein. Two other peptides were synthesized, also containing two Gly residues, GWGIK and LWGIG, did not have the ability to sequester cholesterol as efficiently as LGYGK did. Making the corresponding mutants of gp41 showed that these other two double Gly substitutions resulted in proteins that were much less fusogenic, although they were equally well expressed at the cell surface. The study demonstrates that drastic changes can be made in the LWYIK segment with the retention of a significant fraction of the fusogenic activity, as long as the mutant proteins interact with cholesterol.

The region of the ectodomain of gp41 from HIV adjacent to the transmembrane segment has been termed the membrane proximal external region (MPER). The MPER is rich in Trp residues and is highly conserved among strains of HIV (Fig. 1). This segment has been shown to have an important contribution to fusogenic potency {Salzwedel, 1999 430 /id;Munoz-Barroso, 1999 443 /id;Dimitrov, 2003 547 /id;Huarte, 2008 552 /id;Lorizate, 2008 551 /id}. In addition, a synthetic peptide corresponding to this domain has membrane destabilizing properties (6;7). The presence of the raft-component lipids, sphingomyelin and cholesterol are important for this peptide to be able to destabilize membranes (8;9). The neutralizing antibody,

Corresponding author: R.M. Epand; tel. 905-525-9140 Ext. 22073; FAX: 905-521-1397; E-mail: epand@mcmaster.ca.
[1]These two individuals contributed equally to the project

[†]This work was supported by the Canadian Natural Sciences and Engineering Research Council (grant RGPIN9848-08), the "Ministère de la Région Wallonne" contract n°14540 (PROTMEM). We would also like to thank the "FRSM" (contract n°3.4505.02) for financial support. The work on mutagenesis and HIV-1 fusion was supported by grant R01 AI-33319 from the National Institutes of Health. R.B. is Research Director at the National Funds for Scientific Research of Belgium (FNRS). A.T. is Research Director at the “Institut National de la Sant é et de la Recherche M édicale ” (INSERM France).

4E10, recognizes the MPER domain specifically when it associates with rafts and blocks membrane fusion {Lorizate, 2006 513 /id;Lorizate, 2008 551 /id;Huarte, 2008 552 /id}.

One of the features that connect MPER to raft domains is the presence of the carboxyl-terminal segment of MPER, LWYIK. This segment, when fused to the maltose binding protein was able to bind to cholesteryl-hemisuccinate agarose (11). In addition, N-acetyl-LWYIK-amide has been shown to sequester cholesterol to membrane domains and to insert more deeply into membranes in the presence of cholesterol (12). The requirements for a CRAC domain have been established through analysis of the sequences of several proteins that interact with cholesterol. These proteins were all found to possess a sequence pattern -L/V-$(X)_{(1–5)}$-Y-$(X)_{(1–5)}$-R/K-, in which (-X-)$_{(1–5)}$ represents between one to five residues of any amino acid (13). Thus, the segment LWYIK is a CRAC domain. The fact that LWYIK fulfills the requirements of a CRAC domain may explain its ability to interact with cholesterol. Supporting the suggestion that the CRAC domain, LWYIK of gp41 is responsible for interaction with cholesterol is our finding that the related sequence IWYIK destroys both the CRAC domain as well as cholesterol interactions (14). In addition, the presence of the CRAC domain, LWYIK, appears to facilitate membrane fusion in cells. The L679I mutant, *i.e.* a single conservative mutation that destroys both the CRAC domain as well as cholesterol sequestration, also caused a marked decrease in the fusion of cells expressing the mutant gp41 (14).

The reason LWYIK preferentially interacts with cholesterol compared with several non-CRAC peptide sequences has been suggested to involve their structural flexibility, their position at the interface and their non-covalent bonding with cholesterol. LWYIK, as part of an MPER segment peptide, is found embedded in the membrane (15). This may also result in it being less available for immune surveillance. The segment LWYIK has also been found to be more hydrophobic (16) and to insert more deeply into the membrane than the less active IWYIK (16;17). In the present work we systematically alter the conformational flexibility of LWYIK by substituting and testing all of the possible sequences containing either G, A or P substituted for W and I in LWYIK. The residues W and I are not required to maintain the CRAC motif. All peptides studied for their interactions with lipids were all in the form of N-acetyl-peptide-amides. Peptide sequences should be assumed to be in this form even when not specifically indicated. Among this family of nine peptides, the most active in sequestering cholesterol was LGYGK, demonstrating as had been suggested by *in silico* calculations, that conformational flexibility was a factor favoring interaction with cholesterol (14). We also compared this peptide with two others having substitutions with two additional Gly residues, *i.e.* GWGIK and LWGIG. These later two peptides do not have CRAC sequences and are therefore less likely to interact with cholesterol.

We also examined the effects of mutations in the LWYIK pentapeptide in the context of the entire HIV-1 Env protein, gp41 by determining the ability of the mutated protein to promote cell-cell fusion. This allowed us to correlate changes in the cholesterol sequestering ability of the peptide with its role in fusion when incorporated into the intact protein. We demonstrate that despite the high degree of conservation of the LWYIK segment, the drastically modified mutant W680G,I682G still retains considerable fusogenic activity. Another gp41 mutated in this pentapeptide that has been reported to have considerable fusogenic activity even though it no longer has a CRAC segment is the Y681P mutant (18). Recently, the amino-terminal portion of MPER has been substituted with a membrane perturbing peptide, indolicidin, with partial retention of fusion activity (19). The present study compares the retention of fusion activity with the ability of the C-terminal portion of MPER to sequester cholesterol.

Materials and Methods

Materials

The peptides are all synthesized as N-acetyl-peptide-amides, *i.e.* blocked at the terminal amino and carboxyl groups, respectively. The peptides GWGIK and LWGIG were synthesized by Synbiosci Corporation (Livermore, CA) and purified by HPLC to >95% purity. The peptides LPYPK, LAYPK, LGYPK, LPYAK, LGYAK, LAYAK, LGYGK, LPYGK and LAYGK were synthesized by GL Biochem (Shanghai, China) and purified by HPLC to >95% purity. Phospholipids and cholesterol were purchased from Avanti Polar Lipids (Alabaster, AL).

Preparation of samples for DSC

Phospholipid and cholesterol were codissolved in chloroform/methanol (2/1, v/v). For samples containing peptide, an aliquot of a solution of the peptide in methanol was added to the lipid solution in chloroform/methanol. The solvent was then evaporated under a stream of nitrogen with constant rotation of a test tube so as to deposit a uniform film over the bottom third of the tube. Last traces of solvent were removed by placing the tube under high vacuum for at least three hours. The lipid film was then hydrated with 20 mM PIPES, 1 mM EDTA, 150 mM NaCl with 0.002% NaN_3, pH 7.40 and suspended by intermittent vortexing and heating to 50°C over a period of 2 minutes under argon.

Differential Scanning Calorimetry (DSC)

Measurements were made using a Nano Differential Scanning Calorimeter (Calorimetry Sciences Corporation, Lindon, UT). Each sample was scanned with 2–3 cycles of heating and cooling between 0 and 60 °C. The scan rate was 2°C/min and there was a delay of 5 minutes between sequential scans in a series to allow for thermal equilibration. The features of the design of this instrument have been described (20). DSC curves were analyzed by using the fitting program, DA-2, provided by Microcal Inc. (Northampton, MA) and plotted with Origin, version 5.0.

Membrane partitioning studies

Subsequent to DSC analysis, samples were transferred to 1 mL silanized polycarbonate tubes and centrifuged at 200,000×g (100,000 rpm) for 150 minutes at 25 °C in a Sorvall RC M120 centrifuge. A clear supernatant was collected in silanized glass tubes and the spectra recorded between 350 nm and 250 nm using a Cary 50Bio spectrophotometer. The supernatant from a suspension of lipid without peptide was used as a blank. The absorbance at 280 nm, corrected for the blank and for light scattering was used to calculate the amount of peptide remaining in supernatant, compared with the total concentration of peptide determined by absorbance before the addition of lipid.

Modeling

Structure Properties—A search was made for the most favorable conformation of each of the peptides by using PepLook (21). The energy of peptide conformations is calculated by an all atom description of structures with the addition of van der Waals, electrostatic, internal and external hydrophobicity energy terms. The van der Waals contribution was calculated using the 6–12 Lennard-Jones description of the energy of interactions between unbonded atoms (22). Coulomb's equation was used for electrostatic interactions between unbonded charged atoms with a dielectric 'constant' sigmoidally varying from 1 to 80 for the region between atoms and, using FCPAC partial atomic charges (23). The intramolecular hydrophobicity contribution to stability was calculated using atomic Etr (energy of transfer) and the fractions of atomic surface covered by the atoms in interactions. Seven atomic types are used for calculating Etr (24). When structures are calculated in water, the contribution of solvent is

accounted for by an external hydrophobicity energy term where the solvent-accessible surface of atoms is calculated by the method of Shrake and Rupley with 162 points (25–27). From the 500,000 calculated models, the 99 most stable in most instances or, the 999 most stable in some cases are sorted. The energy of each model is calculated as the sum of the van der Waals and electrostatic terms. Calculations are run in conditions of implicit water, lipids and membrane interface.

Cell-cell fusion

Cell culture—293T or African green monkey kidney COS-1 cells, and TZM-BL cells were used for fusion assays. TZM-BL HeLa-based HIV-1 indicator cells (28) that show a high susceptibility to HIV-1 infection were kindly provided by Tranzyme Inc., Birmingham, Ala. These cells contain reporter genes, luciferase and β-galactosidase, that are expressed in the presence of Tat, under the influence of HIV-1 LTR. Cells were subcultured every 3 to 4 days by trypsinization and maintained in Dulbecco's modified Eagle medium (DMEM) supplemented with 10% fetal bovine serum and antibiotics.

Mutagenesis and plasmid vectors—Mutations of the HIV-1 membrane-proximal external region (MPER) were designed by QuikChange (Stratagene, La Jolla, CA), using an NL4.3 (laboratory-adapted X4 strain) KpnI-BamHI envelope fragment that was cloned into vector pSP72. The mutated envelope fragment was subsequently subcloned into an SV-40-based vector (pSRHS) that expresses Tat and Env (1). Subsequently, the mutated envelope was introduced into the envelope expression vector pCDNA3.1/V5-His-TOPO as per the manufacturer's instructions (Invitrogen, Carlsbad, CA), and employed for Env surface expression studies. All mutations were confirmed by sequencing.

Cell – cell fusion assays—293T or Cos-1 cells were transfected with pCDNA or pSRHS constructs expressing wild-type and mutant HIV-1 envelopes using Fugene 6 transfection reagent (Roche Diagnostics Corporation, Indianapolis, IN). The transfected cells expressing the WT/mutant Env were mixed with TZM-BL cells (1:5 ratio) 20–24 hours post-transfection, and re-plated in 24-well plates. After 20 hours, cell-cell fusion was determined by measuring luciferase activity (Luciferase Assay System, Promega) according to the manufacturer's protocol.

Cell surface expression of Env proteins—At 36–40 hours after transfecting the 293T cells with the pCDNA3.1 vectors encoding WT and mutant Envs , the cells were trypsinized and washed in flow cytometry buffer (PBS with 0.1% BSA and 0.1% NaN_3). The Env molecules on the surface of the 293T cells were fluorescently labelled by incubating 100 μL of harvested 293T cells with 0.5μg/mL of gp120-specific b12 (a gift from Dr. Dennis Burton, Scripps Research Institute, La Jolla, CA) at room temperature for 1 hour. This antibody had been tagged with Alexa Fluor™647 (Invitrogen) according to the manufacturer's instructions. The cell surface expression of Env was evaluated by flow cytometry with FACSCalibur (Becton Dickinson, Franklin Lakes, NJ); the data was analyzed using FloJo software version 8.2 (Tree Star Inc., Ashland, OR) and the mean fluorescence intensity (MFI) calculated from the acquisition of at least 30,000 gated events. Nonspecific background fluorescence due to the secondary antibody was subtracted from the MFIs.

Results

DSC

DSC can be used to assess the effect of peptides on the miscibility of cholesterol and SOPC (29). We have used this method to demonstrate that IWYIK has lower ability to sequester cholesterol than LWYIK (14) and that the peptides AWYIK and VWYIK had intermediate

potencies (30). In this work we compare the effects of several modified versions of LWYIK at 5, 10 or 15 mol% on the phase transition behaviour of SOPC alone or in the presence of 30 or 40 mol% cholesterol.

The phase transition of SOPC in the absence of cholesterol was at 5 °C in cooling scans, with an enthalpy of 4 kcal/mol. Addition of 5, 10 or 15 mol% of any of the peptides studied in this work, except for LWGIG, had no effect on the transition temperature or enthalpy of pure SOPC. The transition temperature of pure SOPC was affected only by the peptide LWGIG that caused a shift to 4.7, 4.7 and 4.5 °C at 5, 10 and 15 mol% peptide, respectfully. We suggest this is a consequence of the lack of charge on this peptide. After centrifugation of the mixtures of SOPC with 5, 10 or 15% of the peptides, all the peptides were found in the supernatant expect for LGYPK for which about 40% of the peptide was bound to the lipid.

DSC curves of a few representative peptides in the presence of SOPC with 30% cholesterol are shown in Figure 2. We compare the effects of the most flexible peptide, LGYGK (top row of Fig. 2) with those of the least flexible in the series, LPYPK (middle row of Fig. 2) and a non-CRAC peptide, GWGIK (bottom row of Fig. 2). There is a large difference in the DSC profile for the scans with LGYGK that have qualitatively larger peaks than those with the least flexible peptide, LPYPK. The shapes of the curves for LGYGK are similar to those of the wild type sequence LWYIK that have been previously published (12). By comparison, the curves at low mol fraction of GWGIK exhibit a broader transition, indicating a less pure SOPC-enriched domain. Differences are also observed when comparing the enthalpy of SOPC with 30 or 40% cholesterol in the presence or absence of the various peptides (Table 1). The precision of the enthalpy values is ± 10%. However, the accuracy is estimated to be ± 15% for the SOPC mixtures with 30% cholesterol and ± 25% for the SOPC mixtures with 40% cholesterol. This is a result of inaccuracies in drawing the baseline on the low temperature side of the transition and is somewhat larger for higher cholesterol mol fractions because of the greater broadness of the transitions. The only peptide not included in this table is LWGIG because it caused a lowering of the transition temperature in these mixtures that did not allow measurement of the full transition peak on cooling. For the remainder of the peptides, there is some similarity in their behaviour, since they all generally exhibit transitions for SOPC that are larger than that of the pure lipid. This is confirmed with the SOPC mixture with 40% cholesterol. However, the differences among the peptides are more clearly revealed in the results from the SOPC mixture with 30% cholesterol (Table 1). For example, peptides with P in the 4^{th} position, including LPYPK, LAYPK and LGYPK, have enthalpies less than 1 kcal/mol for all three concentrations of peptide (with the small exception of LPYPK at 15%, which is just over 1). The non-CRAC peptide, GWGIK also has enthalpies below 1 kcal/mol with this lipid mixture. In comparison the wild type peptide, LWYIK and LGYGK have enthalpies of 1 kcal/mol or greater than 1 for all three peptide concentrations. In particular, at 5 mol% LGYGK is the peptide that exhibits the highest enthalpy for the SOPC transition in the mixture with 30% cholesterol. and in the 40% cholesterol mixture it gives an SOPC peak that has a larger enthalpy than that for the wild type, LWYIK. Curiously, GWGIK produces the largest peaks for the SOPC transition in mixtures with 40% cholesterol, with magnitudes comparable to those observed with 30% cholesterol and little dependence on peptide concentration. It is clear that GWGIK behaves differently with these lipid mixtures than do the other peptides.

Another consequence of the formation of cholesterol-rich domains can be that the sterol passes its solubility limit in a region of the membrane, forming crystallites. Anhydrous crystalline cholesterol is known to undergo a crystalline polymorphic phase transition at 38 °C on heating and at 23 °C on cooling at a scan rate of 2°/min (31), with an enthalpy of 910 cal/mol (32). This hysteresis is characteristic of anhydrous cholesterol crystals and provides a criterion for identifying the presence of these crystals. There are no cholesterol crystals found in the absence of peptide, even up to a ratio of 1:1 SOPC:cholesterol. At SOPC/cholesterol molar ratios of

7/3 and 6/4, most of the peptides induce the formation of cholesterol crystals corresponding to about 4, 5 or 10% of the total amount of cholesterol at 5, 10 and 15% peptide, respectively. The polymorphic transition of anhydrous cholesterol crystallites can be just discerned for LPYPK in Fig. 2. It is also evident in scans with LGYGK using 40% cholesterol in SOPC (not shown). The only peptide that does not exhibit cholesterol crystallites is LWGIG that shows no formation of anhydrous cholesterol crystals at any of the SOPC/cholesterol ratios. It was mentioned above that LWGIG was the only peptide to affect the transition of pure SOPC. This combined with the lack of formation of cholesterol crystallites suggest that this peptide does not preferentially interact with either cholesterol or SOPC in mixtures of the two lipids. In addition, the peptide GWGIK shows no formation of cholesterol crystals at a 6/4 ratio of SOPC/cholesterol also suggesting that there may be only a weak preferential interaction of this peptide with one of these two lipids. However, there is a small peak corresponding to cholesterol crystals in the mixtures of this peptide with 30% cholesterol (Fig. 2). This is another indication of the unusual behaviour of the interaction of this peptide with SOPC/cholesterol mixtures. Thus, the two non-CRAC peptides have the least tendency to preferentially interact with cholesterol. It should be pointed out, however, that cholesterol crystals could form if the peptide preferentially interacted with the SOPC component, resulting in cholesterol being removed from this domain. Hence we do not consider the formation of cholesterol crystallites as good evidence for preferential binding of peptides to cholesterol. However, the converse is true, *i.e.* that lack of cholesterol crystallite formation is useful as an indication of the lack of preferential interaction of the peptide with cholesterol.

For all three mixtures of SOPC in the presence of cholesterol almost all of the peptides were found bound to the lipid pellet after centrifugation. This indicates that differences in membrane partitioning among the peptides studied had only a minor effect on their ability to affect the phase transitions of the lipid mixtures. It also shows that cholesterol increases the partitioning of these peptides to the membrane compared with pure SOPC.

Modeling

3D structures of the peptides were calculated in conditions of hydrophilic, interfacial and hydrophobic media. We used Peplook to calculate the peptide structural possibilities (Fig. 3). Analyses of the RMS deviation of the 99 PepLook models demonstrate that the LGYGK peptide has the largest plasticity with a RMS deviation up to 4 Å, the most constrained peptide being LPYPK. When we sort the 999 PepLook models of lower energy at the membrane interface and rank them by delta energy (Fig. 4), we notice that LWYIK has a wider energy distribution than LPYPK. Therefore, LPYPK is both structurally and energetically restricted, LGYGK has wider structural and energy possibilities, and LWYIK with intermediate structural possibilities has the best capacity of energy stabilization. This demonstrates that LWYIK is the peptide that shows the greatest stability at a membrane interface.

Mutagenesis of the membrane-proximal external region (MPER) of HIV-1 gp41

We examined the effects of mutations in the LWYIK segment in the context of the entire HIV-1 Env. This peptide is part of the HIV-1 MPER in the gp41 ectodomain whose crucial role in viral fusion has been established (1). We employed the QuikChange mutagenesis method to generate mutants in which two Glycine residues were substituted in the LWYIK segment of MPER. The following mutants were made (sequences in parenthesis show the modified form of the LWYIK segment that was generated and is the way these mutants will be referred to below): L679G, Y681G (GWGIK); Y681G, K683G (LWGIG) and W680G, I 682G (LGYGK).

Effects on cell-cell fusion

The fusion efficiency of LGYGK was somewhat less than the wild type, but was much greater than for LWGIG or GWGIK (Fig. 5).

Cell surface expression of Env proteins

There is only a small reduction of about 10% in cell surface expression of any of the mutants, relative to the wild-type protein taken as 100% (Fig. 6).

Discussion

We have shown previously that the peptide LWYIK promoted the segregation of membrane lipids into cholesterol-rich and cholesterol-poor domains. Evidence for the formation of a domain depleted of cholesterol came from DSC, which exhibited a more cooperative and higher enthalpy gel to liquid crystalline phospholipid phase transition. Apparently the other regions of the membrane that are enriched in cholesterol have a sufficiently high cholesterol concentration that they pass the solubility limit of cholesterol in the membrane, forming cholesterol crystallites (12). In addition, the presence of cholesterol was shown to allow a greater depth of penetration of LWYIK into the membrane bilayer (17). In the present study we introduced amino acid substitutions that would be expected to drastically alter the conformational flexibility of LWYIK. Gly has the smallest side chain and is expected to allow the greatest amount of conformational flexibility, while Pro is the most conformationally restricted because of its ring structure and Ala is of intermediate flexibility.

LWYIK represents a CRAC sequence (13). According to the CRAC algorithm, the second and fourth residue of LWYIK can be substituted with any amino acid while maintaining the peptide as a CRAC sequence. We studied a series of peptides with the W and I residues substituted with A, P or G. Hence, all of the modified sequences correspond to CRAC segments. In addition, we studied GWGIK and LWGIG that also have two amino acid substitutions in LWYIK but these two peptides are not CRAC sequences. We find that all of the CRAC sequences, and even GWGIK induce increased enthalpy of the SOPC transition in mixtures of SOPC and cholesterol (Table 1). However, the non-CRAC sequences GWGIK and LWGIG behave differently. LWGIG is the only peptide of the series to affect the phase transition of pure SOPC. In addition, this peptide has the largest effect in lowering the temperature of the transition of mixtures of SOPC with cholesterol. Furthermore, LWGIG is the only peptide that does not promote the formation of cholesterol crystals in mixtures of SOPC with either 30 or 40% cholesterol. GWGIK also has unique properties. It exhibits the highest transition enthalpy with mixtures of SOPC and 40% cholesterol, but these enthalpies are similar to those observed with this peptide in mixtures containing 30% cholesterol. Unlike the wild type LWYIK, there is no increase in the enthalpy of this transition with increasing peptide concentration. In addition, GWGIK induces cholesterol crystallite formation with mixtures of SOPC and 30% cholesterol, but curiously not with 40% cholesterol. These non-CRAC peptides have a qualitatively different behaviour from the others.

Among the CRAC peptides, the one that induces a somewhat greater enthalpy for the SOPC transition (Table 1) is the sequence LGYGK. We have therefore introduced these two amino acid substitutions into the LWYIK segment of the intact Env protein by substituting W^{680} and I^{682} with G. We find that expression of the resultant mutant protein supports 72% of the fusion activity of the WT protein (Fig. 5). It is remarkable that two such non-conservative substitutions could be introduced into an invariant region of the HIV-1 gp41, with only a relatively modest lost of fusion activity. It has recently been demonstrated that a large segment of the MPER region can be replaced with a sequence of amino acids corresponding to a membrane-perturbing peptide (19). The more active mutants retained the segment WYIK and had only partial fusogenic activity. It remains to be determined how important the LWYIK segment is for full fusion activity and for cholesterol recognition in these constructs. The finding that the peptide LGYGK retained considerable activity in segregating cholesterol in model membranes combined with the observation that introduction of this sequence in the intact gp41 protein allowed considerable retention of fusogenic activity is good evidence that there is a correlation

between the ability of this region of the protein to sequester to a cholesterol-rich region and its infectivity.

Thus, when one compares mutants with similar kinds of substitutions, such as the I^{679}, V^{679} and A^{679} or for the group of three mutants described in this manuscript with the substitution of 2 Gly residues, there is good correlation between reorganization of cholesterol in model membranes by the corresponding peptide and the fusogenicity of the virus. However, the interaction with cholesterol is not the only factor determining the fusogenic activity of the mutant forms of gp41. Thus, the L679I mutant has about the same fusogenic activity as does the W680G, I682G mutant. Nevertheless, the peptide LGYGK is much more effective in sequestering cholesterol (Table 1) than is the peptide IWYIK (30). This supports the CRAC hypothesis for cholesterol interactions since LGYGK is a CRAC sequence but IWYIK is not. Although LGYGK has a stronger interaction with cholesterol than IWYIK, L679I and the W680G, I682G gp41 mutants have comparable fusogenic activity. Changing L to I involves only moving a methyl group from one carbon atom to another, while the W680G, I682G mutant replaces two hydrophobic, bulky residues with two that are small, conformationally flexible and not hydrophobic in a region of gp41 that is invariant. There are likely other factors, in addition to the interaction with cholesterol that will determine the biological properties of these mutants. Nevertheless, within a similar series of mutations the correlation between the peptide affecting cholesterol distribution and the fusogenic activity of the mutant gp41 is good. In addition, the fact that we can make a drastic change in the LWYIK segment of gp41, and still retain considerable fusogenic activity as well as cholesterol sequestering ability (with the W680G, I682G mutant), is good evidence that interactions of this region of the protein with cholesterol play an important, but not unique role, in viral fusion.

An indication that cholesterol is important for the membrane interactions of HIV is the finding that the cholesterol/phospholipid ratios in the viral membrane of HIV are generally higher than that of the host membranes (33), although the exact increase varies from strain to strain and also depends on other factors including the growth conditions and the type of target cell used. It has been suggested that the HIV envelop has a lipid composition suggesting that it has raft-like properties (34). HIV viral membrane proteins have also been shown to sequester into cholesterol-rich raft domains in the membrane during viral assembly (35). Cell membrane raft domains are important for viral entry and assembly (36). Cholesterol may be particularly important for viral fusion and internalization since these processes are inhibited by lower viral membrane cholesterol even though membrane binding is not inhibited (37). Similar to cholesterol depletion, mutations in the MPER region that would be expected to reduce cholesterol affinity lead to reduced fusion. The presence of the CRAC segment will allow the virus to sequester itself into specific host cholesterol domains and bud out of the cell, presumably containing an optimal amount of cholesterol in its own membrane.

It is also interesting to consider how cholesterol could affect the interaction of the intact HIV with membranes since there has been some imaging of the native structure of Env on the surface of the virion. One study proposed a splayed-legs model for Env wherein the Env trimer positions itself in the viral membrane like a tripod (38). This model suggests extensive interaction of gp41 molecules with the viral membrane, and possible interaction of the Env with cholesterol-rich membrane domain on the target cell membrane. This could affect Env stability and subsequent internalization. However, there is an alternate model (39) in which a compact stalk-like Env structure interacts with membranes. In this model there is less interaction of gp41 monomers with the membrane, more with each other. For this model it is difficult to visualize the possible affects of modifications of the CRAC segment on viral entry.

Our results indicate that the CRAC domain is important for gp41-induced cell-cell fusion. It is not certain what its importance is for viral-cell fusion. Based on the model presented by (38), it would be likely that this lipid interaction also has a role in virus-cell fusion.

Abbreviations used

MPER, the membrane-proximal external region; CRAC, Cholesterol Recognition/interaction Amino acid Consensus; HIV, human immunodeficiency virus; PC, phosphatidylcholine; SOPC, 1-stearoyl-2-oleoyl phosphatidylcholine; DSC, differential scanning calorimetry; T_m, phase transition temperature; ΔH, calorimetric enthalpy; MFP, Mean Force Potential; MFI, mean fluorescence intensity.

References

1. Salzwedel K, West JT, Hunter E. A conserved tryptophan-rich motif in the membrane-proximal region of the human immunodeficiency virus type 1 gp41 ectodomain is important for Env-mediated fusion and virus infectivity. J. Virol 1999;73:2469–2480. [PubMed: 9971832]
2. Munoz-Barroso I, Salzwedel K, Hunter E, Blumenthal R. Role of the membrane-proximal domain in the initial stages of human immunodeficiency virus type 1 envelope glycoprotein-mediated membrane fusion. J. Virol 1999;73:6089–6092. [PubMed: 10364363]
3. Dimitrov AS, Rawat SS, Jiang S, Blumenthal R. Role of the fusion peptide and membrane-proximal domain in HIV-1 envelope glycoprotein-mediated membrane fusion. Biochemistry 2003;42:14150–14158. [PubMed: 14640682]
4. Huarte N, Lorizate M, Maeso R, Kunert R, Arranz R, Valpuesta JM, Nieva JL. The broadly neutralizing anti-HIV-1 4E10 monoclonal antibody is better adapted to membrane-bound epitope recognition and blocking than 2F5. J Virol 2008;82:8986–8996. [PubMed: 18596094]
5. Lorizate M, Huarte N, Saez-Cirion A, Nieva JL. Interfacial pre-transmembrane domains in viral proteins promoting membrane fusion and fission. Biochim. Biophys. Acta 2008;1778:1624–1639. [PubMed: 18222166]
6. Suarez T, Gallaher WR, Agirre A, Goni FM, Nieva JL. Membrane interface-interacting sequences within the ectodomain of the human immunodeficiency virus type 1 envelope glycoprotein: putative role during viral fusion. J. Virol 2000;74:8038–8047. [PubMed: 10933713]
7. Suarez T, Nir S, Goni FM, Saez-Cirion A, Nieva JL. The pre-transmembrane region of the human immunodeficiency virus type-1 glycoprotein: a novel fusogenic sequence. FEBS Lett 2000;477:145–149. [PubMed: 10899326]
8. Saez-Cirion A, Nir S, Lorizate M, Agirre A, Cruz A, Perez-Gil J, Nieva JL. Sphingomyelin and cholesterol promote HIV-1 gp41 pretransmembrane sequence surface aggregation and membrane restructuring. J. Biol. Chem 2002;277:21776–21785. [PubMed: 11929877]
9. Shnaper S, Sackett K, Gallo SA, Blumenthal R, Shai Y. The C-and the N-terminal regions of glycoprotein 41 ectodomain fuse membranes enriched and not enriched with cholesterol, respectively. J. Biol. Chem 2004;279:18526–18534. [PubMed: 14981088]
10. Lorizate M, Cruz A, Huarte N, Kunert R, Perez-Gil J, Nieva JL. Recognition and Blocking of HIV-1 gp41 Pre-transmembrane Sequence by Monoclonal 4E10 Antibody in a Raft-like Membrane Environment. J. Biol. Chem 2006;281:39598–39606. [PubMed: 17050535]
11. Vincent N, Genin C, Malvoisin E. Identification of a conserved domain of the HIV-1 transmembrane protein gp41 which interacts with cholesteryl groups. Biochim. Biophys. Acta 2002;1567:157–164. [PubMed: 12488049]
12. Epand RM, Sayer BG, Epand RF. Peptide-induced formation of cholesterol-rich domains. Biochemistry 2003;42:14677–14689. [PubMed: 14661981]
13. Li H, Papadopoulos V. Peripheral-type benzodiazepine receptor function in cholesterol transport. Identification of a putative cholesterol recognition/interaction amino acid sequence and consensus pattern. Endocrinology 1998;139:4991–4997. [PubMed: 9832438]

14. Epand RF, Thomas A, Brasseur R, Vishwanathan SA, Hunter E, Epand RM. Juxtamembrane protein segments that contribute to recruitment of cholesterol into domains. Biochemistry 2006;45:6105–6114. [PubMed: 16681383]
15. Sun ZY, Oh KJ, Kim M, Yu J, Brusic V, Song L, Qiao Z, Wang JH, Wagner G, Reinherz EL. HIV-1 Broadly Neutralizing Antibody Extracts Its Epitope from a Kinked gp41 Ectodomain Region on the Viral Membrane. Immunity 2008;28:52–63. [PubMed: 18191596]
16. Greenwood AI, Pan J, Mills TT, Nagle JF, Epand RM, Tristram-Nagle S. CRAC motif peptide of the HIV-1 gp41 protein thins SOPC membranes and interacts with cholesterol. Biochim. Biophys. Acta 2008;1778:1120–1130. [PubMed: 18262490]
17. Epand RM, Hughes DW, Sayer BG, Borochov N, Bach D, Wachtel E. Novel properties of cholesterol-dioleoylphosphatidylcholine mixtures. Biochim. Biophys. Acta 2003;1616:196–208. [PubMed: 14561477]
18. Cao J, Bergeron L, Helseth E, Thali M, Repke H, Sodroski J. Effects of amino acid changes in the extracellular domain of the human immunodeficiency virus type 1 gp41 envelope glycoprotein. J. Virol 1993;67:2747–2755. [PubMed: 8474172]
19. Vishwanathan SA, Hunter E. Importance of its Membrane-Perturbing Properties of the Membrane-Proximal External Region of Human Immunodeficiency Virus Type 1 gp41 to Viral Fusion. J. Virol 2008;82:5118–5126. [PubMed: 18353966]
20. Privalov G, Kavina V, Freire E, Privalov PL. Precise scanning calorimeter for studying thermal properties of biological macromolecules in dilute solution. Anal. Biochem 1995;232:79–85. [PubMed: 8600837]
21. Thomas A, Deshayes S, Decaffmeyer M, Van Eyck MH, Charloteaux B, Brasseur R. Prediction of peptide structure: how far are we? Proteins 2006;65:889–897. [PubMed: 17019719]
22. Lins L, Brasseur R, De Pauw M, Van Biervliet JP, Ruysschaert JM, Rosseneu M, Vanloo B. Helix-helix interactions in reconstituted high-density lipoproteins. Biochim. Biophys. Acta 1995;1258:10–18. [PubMed: 7654775]
23. Leach, AR. van der Waals Interactions. In: Leach, AR., editor. Molecular Modelling: Principles and Applications. Harlow, England: Longman Ltd.; 1996. p. 171-177.
24. Moult J, James MN. An algorithm for determining the conformation of polypeptide segments in proteins by systematic search. Proteins 1986;1:146–163. [PubMed: 3130622]
25. Thomas A, Milon A, Brasseur R. Partial atomic charges of amino acids in proteins. Proteins 2004;56:102–109. [PubMed: 15162490]
26. Brasseur R. Simulating the folding of small proteins by use of the local minimum energy and the free solvation energy yields native-like structures. J Mol. Graph 1995;13:312–322. [PubMed: 8603060]
27. Lins L, Thomas A, Brasseur R. Analysis of accessible surface of residues in proteins. Protein Sci 2003;12:1406–1417. [PubMed: 12824487]
28. Wei X, Decker JM, Liu H, Zhang Z, Arani RB, Kilby JM, Saag MS, Wu X, Shaw GM, Kappes JC. Emergence of resistant human immunodeficiency virus type 1 in patients receiving fusion inhibitor (T-20) monotherapy. Antimicrob. Agents. Chemother 2002;46:1896–1905. [PubMed: 12019106]
29. Epand RM. Detecting the presence of membrane domains using DSC. Biophys. Chem 2007;126:197–200. [PubMed: 16730877]
30. Vishwanathan SA, Thomas A, Brasseur R, Epand RF, Hunter E, Epand RM. Hydrophobic Substitutions in the First Residue of the CRAC Segment of the gp41 Protein of HIV. Biochemistry 2008;47:124–130. [PubMed: 18081318]
31. Epand RM, Bach D, Borochov N, Wachtel E. Cholesterol crystalline polymorphism and the solubility of cholesterol in phosphatidylserine. Biophys. J 2000;78:866–873. [PubMed: 10653799]
32. Loomis CR, Shipley GG, Small DM. The phase behavior of hydrated cholesterol. J. Lipid Res 1979;20:525–535. [PubMed: 458269]
33. Aloia RC, Tian H, Jensen FC. Lipid composition and fluidity of the human immunodeficiency virus envelope and host cell plasma membranes. Proc. Natl. Acad. Sci. U. S. A 1993;90:5181–5185. [PubMed: 8389472]
34. Brugger B, Glass B, Haberkant P, Leibrecht I, Wieland FT, Krausslich HG. The HIV lipidome: a raft with an unusual composition. Proc. Natl. Acad. Sci. U. S. A 2006;103:2641–2646. [PubMed: 16481622]

35. Leung K, Kim JO, Ganesh L, Kabat J, Schwartz O, Nabel GJ. HIV-1 assembly: viral glycoproteins segregate quantally to lipid rafts that associate individually with HIV-1 capsids and virions. Cell Host. Microbe 2008;3:285–292. [PubMed: 18474355]

36. Luo C, Wang K, Liu dQ, Li Y, Zhao QS. The functional roles of lipid rafts in T cell activation, immune diseases and HIV infection and prevention. Cell Mol Immunol 2008;5:1–7. [PubMed: 18318989]

37. Guyader M, Kiyokawa E, Abrami L, Turelli P, Trono D. Role for human immunodeficiency virus type 1 membrane cholesterol in viral internalization. J Virol 2002;76:10356–10364. [PubMed: 12239312]

38. Zhu P, Liu J, Bess J Jr, Chertova E, Lifson JD, Grise H, Ofek GA, Taylor KA, Roux KH. Distribution and three-dimensional structure of AIDS virus envelope spikes. Nature 2006;441:847–852. [PubMed: 16728975]

39. Zanetti G, Briggs JA, Grunewald K, Sattentau QJ, Fuller SD. Cryo-electron tomographic structure of an immunodeficiency virus envelope complex in situ. PLoS. Pathog 2006;2:e83. [PubMed: 16933990]

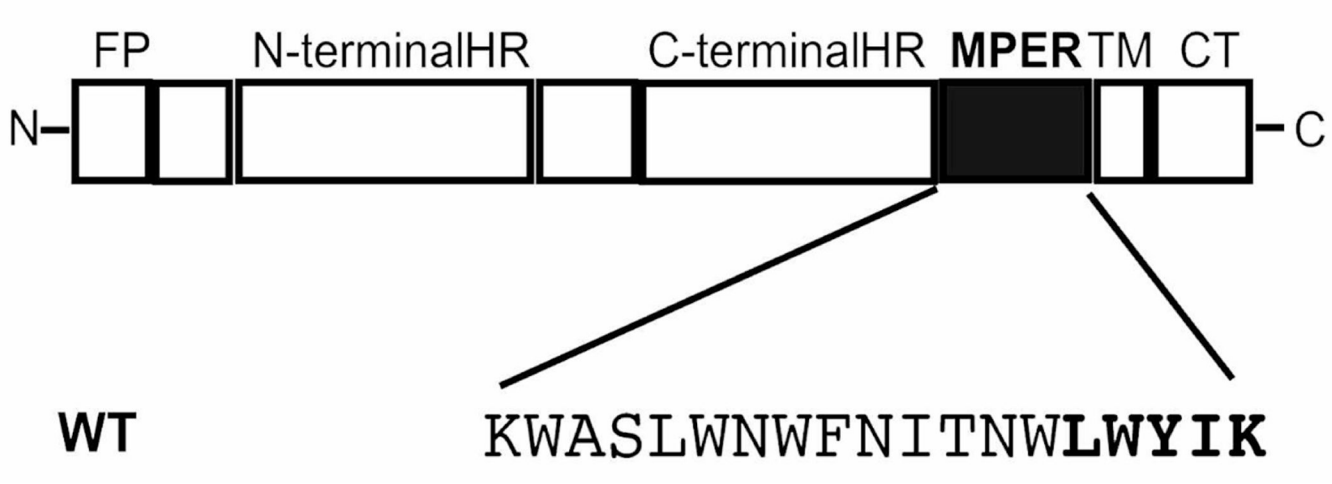

Figure 1.
Schematic representation of HIV-1 gp41. The sequence of MPER is shown with the C-terminal CRAC segment, LWYIK, highlighted. MPER lies between the C-terminal heptad repeat (HR) and the transmembrane (TM) region. FP, fusion peptide; CT, cytoplasmic tail.

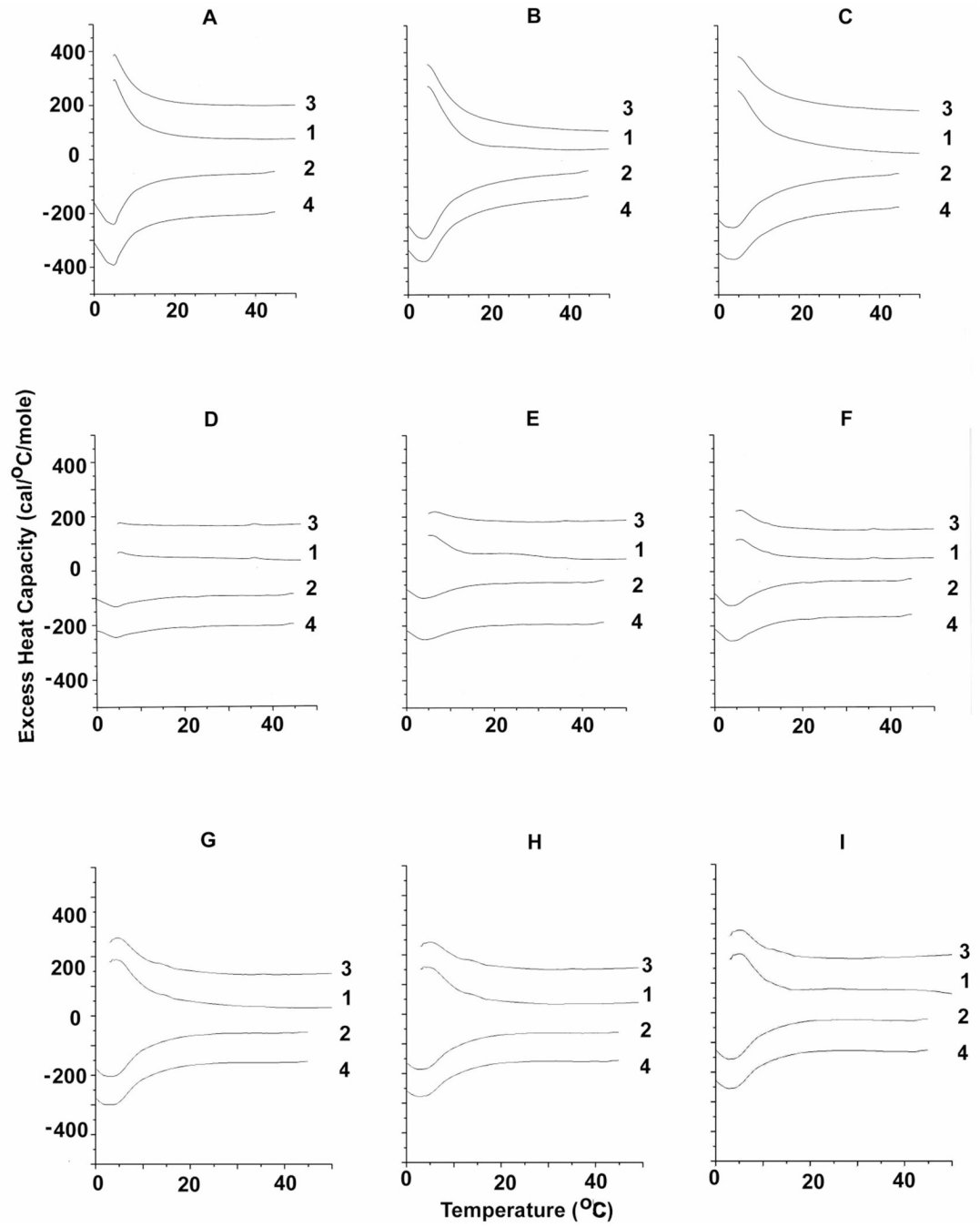

Figure 2.

Differential scanning calorimetry of SOPC with 30 mol% cholesterol. Scan rate 2K/min. Lipid concentration 2.5 mg/mL in 20 mM PIPES, 1 mM EDTA, 150 mM NaCl with 0.002% NaN_3, pH 7.40. Sequential heating and cooling scans between 0 and 50 °C. Numbers are the order in which the scans were carried out, with scans 1 and 3 being heating scans, each of which was followed by one of the cooling scans 2 or 4. Scans were displaced along the y-axis for clarity of presentation. N-acetyl-LGYGK-amide is added to samples whose DSC is shown in panels A, B and C; N-acetyl-LPYPK-amide in panels D, E and F; N-acetyl-GWGIK-amide in panels G, H and I. Peptide content is 5 mol % for panels A, D and G; 10 mol % for panels B, E and H and 15 mol % for panels C, F and I.

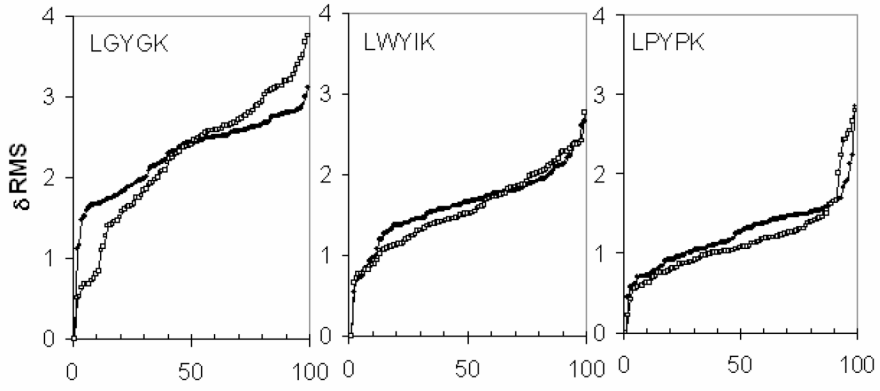

Figure 3.

RMS variation of the LWYIK, LGYGK and LPYPK models calculated by PepLook (21). Models are calculated in hydrophobic (□) and hydrophilic (•) conditions. At the end of the iterative PepLook process, 99 models of lower energy were sorted. They are plotted by their variation in RMS by reference to the structure of the Prime.

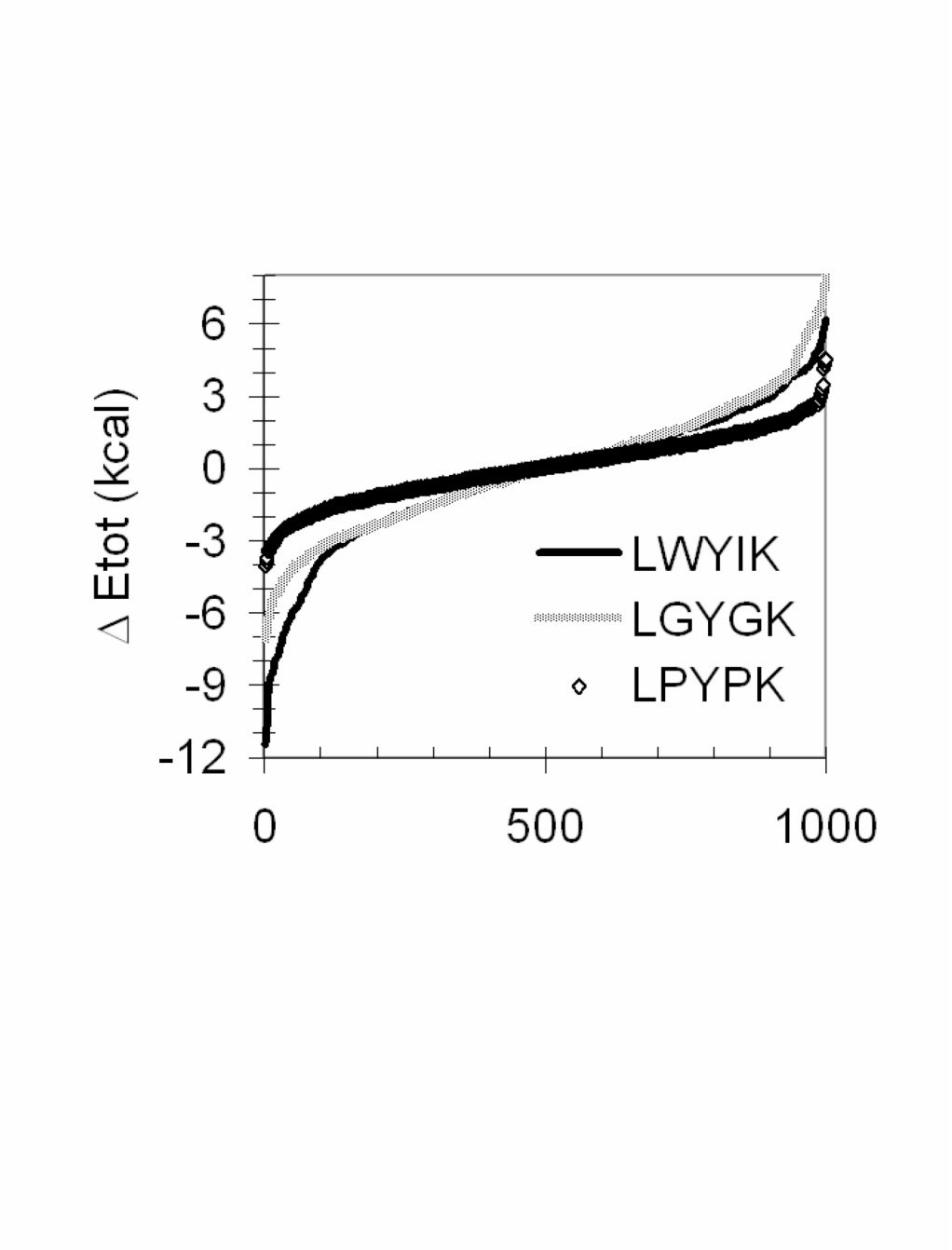

Figure 4.
Energy variation of the models of LWYIK, LGYGK and LPYPK calculated by PepLook (21). At the end of the iterative calculation process, 999 models instead of 99 models of lower energy were sorted. They are plotted by their variation in energy by reference to 500th model of the population. Energy are sum of van der Waals and electrostatic contributions.

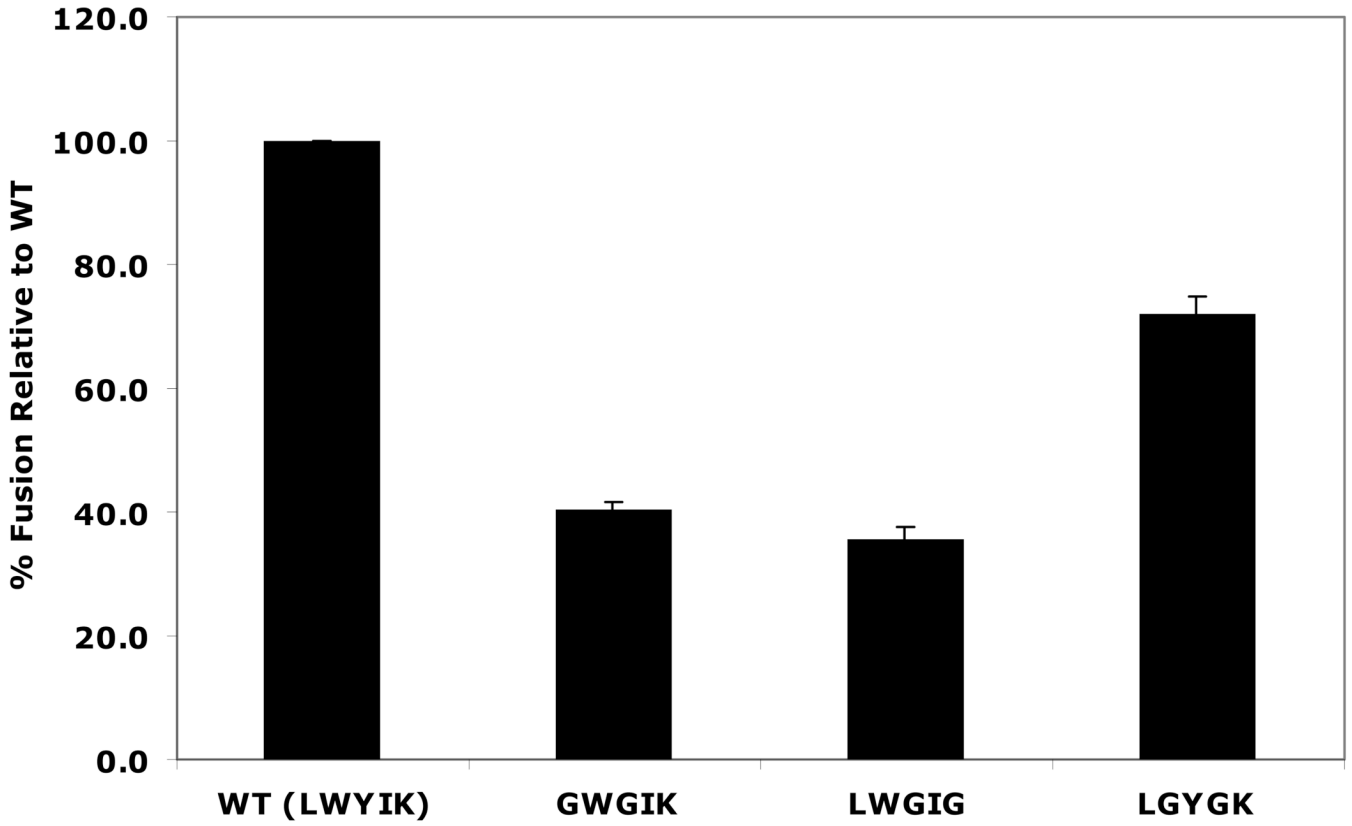

Figure 5.
Cell-cell fusion assays of wild-type (WT) and MPER mutants GWGIK, LWGIG and LGYGK. Data shown is the average of four experiments (with transfected Cos-1 cells), for each of which samples were run in duplicate. Luciferase activity (RLU, relative light units) was determined as per the manufacturer's instructions, and normalized as a percentage of that observed with the wild-type.

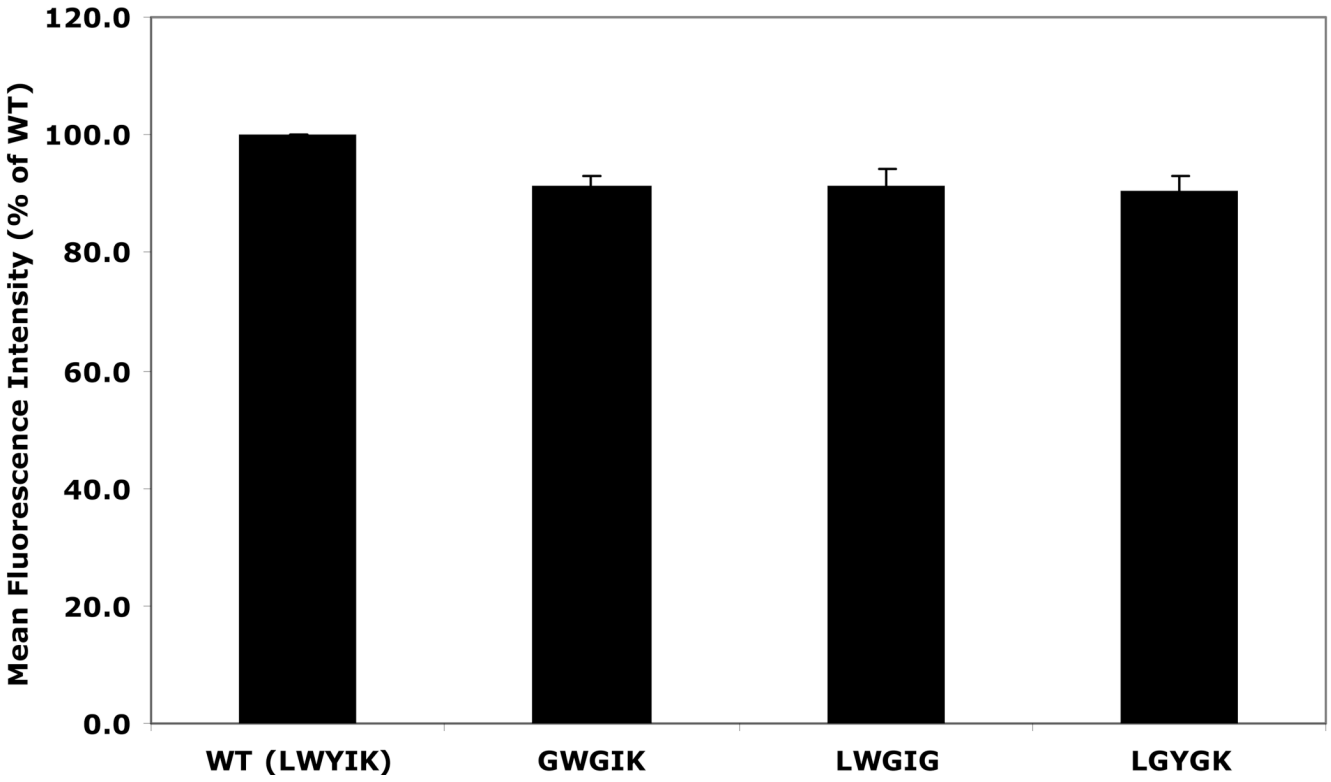

Figure 6.
Cell surface expression (measured by calculating the mean fluorescence intensity, MFI) of mutant and WT Env proteins. The results indicate the expression of mutant Env on the surface of 293T cells as a percentage of WT.

Table 1

Enthalpies of the Chain Melting Transition of SOPC

Mol % Peptide	Peptide	ΔH (kcal/mol)	
		7/3 SOPC/cholesterol	6/4 SOPC/cholesterol
0	None	0.52	0.1
5	LWYIK	1.0	0.1
10		1.1	0.3
15		1.4	0.5
5	LPYPK	0.4	0.2
10		0.5	0.3
15		1.1	0.4
5	LAYAK	0.4	0.3
10		0.6	0.6
15		1.0	0.5
5	LGYGK	1.5	0.2
10		1.4	0.3
15		1.2	0.3
5	LPYAK	1.1	0.3
10		1.4	0.3
15		1.1	0.4
5	LAYPK	0.5	0.3
10		0.6	0.4
15		0.9	0.4
5	LPYGK	0.8	0.2
10		1.5	0.3
15		1.3	0.4
5	LGYPK	0.6	0.3
10		0.3	0.4
15		0.8	0.4
5	LAYGK	0.9	0.2
10		1.0	0.2
15		1.0	0.3
5	LGYAK	0.7	0.2
10		0.5	0.2
15		0.8	0.1
5	GWGIK	0.9	0.5
10		0.8	0.7
15		0.7	0.9